



HAL
open science

Gas Adsorption Evidence of Single-Wall and Multi-Wall Carbon Nanotube Opening

Moulay-Rachid Babaa, Edward Merae, Nicole Dupont-Pavlovsky, Sandrine Delpeux, Francois Beguin, Fabrice Valsaque, Jaafar Ghanbaja

► **To cite this version:**

Moulay-Rachid Babaa, Edward Merae, Nicole Dupont-Pavlovsky, Sandrine Delpeux, Francois Beguin, et al.. Gas Adsorption Evidence of Single-Wall and Multi-Wall Carbon Nanotube Opening. MRS Online Proceedings Library, 2011, 782 (A9.5), 10.1557/PROC-782-A9.5 . hal-03313565

HAL Id: hal-03313565

<https://hal.science/hal-03313565>

Submitted on 6 May 2023

HAL is a multi-disciplinary open access archive for the deposit and dissemination of scientific research documents, whether they are published or not. The documents may come from teaching and research institutions in France or abroad, or from public or private research centers.

L'archive ouverte pluridisciplinaire **HAL**, est destinée au dépôt et à la diffusion de documents scientifiques de niveau recherche, publiés ou non, émanant des établissements d'enseignement et de recherche français ou étrangers, des laboratoires publics ou privés.

Gas Adsorption Evidence of Single-Wall and Multi-Wall Carbon Nanotube Opening

Moulay-Rachid Babaa¹, Edward McRae¹, Nicole Dupont-Pavlovsky¹, Sandrine Delpoux², Francois Beguin², Fabrice Valsaque¹, Jaafar Ghanbaja¹.

¹ Laboratoire de Chimie du Solide Minéral, UMR CNRS 7555, Université Henri Poincaré – Nancy 1, B.P. 239, 54506 Vandoeuvre cedex, France

² Centre de Recherche sur la Matière Divisée, CNRS-Université, 1b rue de la Férollerie, 45071 Orléans cedex 02, France

ABSTRACT

Carbon nanotubes offer a surface very similar to that of graphite, a reference substrate in physisorption experiments aimed at studying substrate-adsorbate interactions. The curvature, however, introduces new questions. What are the effects of this on condensation pressures or heats of adsorption? Can one experimentally distinguish between different adsorption sites? In this study, we compare adsorption isotherms of several simple gases (Kr, Xe, CCl₄) on single-wall (SWNTs) and multi-wall carbon nanotubes (MWNTs), before and after opening. For mechanically opened SWNTs, the accessibility of the adsorption sites and the molecular arrangements of the adsorbed gases are discussed. With the much bigger, well-defined MWNTs, the “cutting method” called upon a nitric acid treatment followed by a CO₂ oxidation. TEM investigations and physisorption studies clearly revealed tube opening and that the inner channels became accessible to Kr molecules.

INTRODUCTION

Since the early research works on carbon nanotubes (CNTs), effort has been made to open nanotubes so as to encapsulate elements and molecules [1]. This has allowed creating 1D wires and showing the existence of various compounds with structural parameters different than those of bulk 3D materials [2, 3] because of the confinement. Over the past years, several theoretical studies have further suggested that adsorption might take place inside the tubes if they could be opened. The present study shows that opening tubes can indeed be done and that evidence is provided by adsorption isotherms.

A physisorption isotherm of simple molecules on a uniform surface such as graphite displays vertical steps representative of 2D phase transitions corresponding to the deposition of successive monomolecular layers. Concerning CNTs, which consist of coaxially rolled, seamless graphene sheets, two steps can be distinguished in simple gas adsorption isotherms which result from the condensation of the adsorbed phase on the uniform patches of the outer surface. In the case of closed SWNTs, which are organized in bundles, the first step has been attributed to adsorption in the grooves and the largest interstitial channels, and the second has been assigned to adsorption on the external convex surface of the individual outermost tubes making up the bundle [4,5,6]. In the case of closed MWNTs, both steps are thought to represent successive condensations on the external surface of the nanotubes [7,8]. In this paper, we show that it is possible, using adsorption measurements coupled with TEM observations, to give evidence of tube opening and to estimate the surface modifications resulting from the opening techniques.

EXPERIMENTAL DETAILS

Volumetric measurements

Adsorption isotherms were performed from the very first stages of adsorption ($P/P_0 \approx 10^{-6}$, where P is the pressure of the gas and P_0 its saturated vapor pressure at the experimental temperature) to the adsorbate saturated vapor pressure. The experimental set-up and cryogenic system are described elsewhere [9]. The cell temperature was maintained constant and uniform to within 0.05 K during each experiment. The isotherm determinations were performed in a classical apparatus equipped with a McLeod and a Datametrics pressure gauge allowing measurement from 10^{-4} to 1300 Pa. Thermal transpiration was taken into account using the semi-empirical equation of Takaishi and Sensui [10]. Before each experiment, the sample was outgassed under a vacuum better than 10^{-4} Pa for at least 6 hours at 873 K.

As-produced and cut nanotube samples

The SWNTs were provided by the GDCP laboratory of Montpellier University (France). They were prepared by means of a Ni-Y catalyzed electric arc discharge method under He atmosphere [11]. The tubes are arranged in bundles, the bundle diameter ranging from 5 to 20 nm. The average tube diameter is around 1.3 nm. SWNTs were cut mechanically by rubbing a pristine sample between two diamond lapping disks [12]. The size of the diamond grains on the disk surface is 0.1 μm . Figure 1 shows a transmission electron microscopy (TEM) photo of a SWNT bundle after the cutting treatment (photo from Ref [12]).

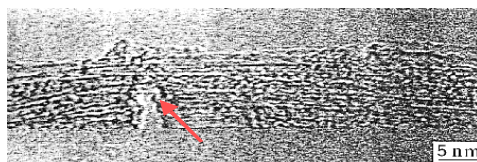


Figure 1. TEM micrograph of a bundle of SWNTs after mechanical opening

The MWNTs used in this work (CRMD Laboratory, Orléans) were prepared by decomposition of acetylene at 600 °C on Co particles from solid state solution ($\text{Co}_x\text{Mg}_{(1-x)}\text{O}$) as described elsewhere [13]. The samples were purified using concentrated HCl and then annealed at 2400°C under flowing Ar. According to TEM observations, the tubes are closed at both ends; their external diameters range from 10 to 45 nm. Opening was performed using HNO_3 treatment and then by CO_2 oxidation [14]. Figure 2 displays TEM images of the sample before and after 40% and 60% burn offs. It is seen that the tubular morphology is preserved but the ends became uncapped after oxidation.

RESULTS AND DISCUSSION

Gas adsorption on as-produced and cut SWNTs

Figure 3a displays adsorption isotherms of Kr, Xe and CCl_4 at 77 K, 110 K and 224 K respectively, The isotherms are normalized to the weight of the sample and represented on a semi-logarithmic scale. All curves show the two steps described above. Figure 3b compares the adsorption isotherms of Kr at 77 K for closed and opened SWNTs. Similar changes are

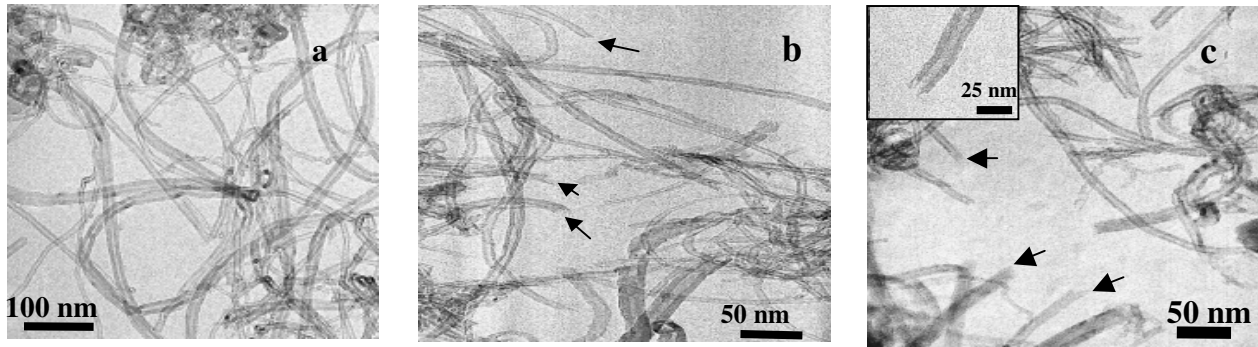


Figure 2. TEM micrograph of MWNTs: (a) pristine sample; (b) oxidized sample 40% burn-off; (c) Oxidized sample 60% burn-off. Arrows indicate some opened ends.

observed for all adsorbates. Two steps on the isotherms are still observable after the cutting process. The main changes in the curves upon tube opening are the appearance of an additional adsorbed amount at the first stages of adsorption and a significant decrease in the first step pressure. The first step after tube opening thus corresponds to adsorption inside the tubes coupled with that in grooves and in the largest interstitial channels.

The pressure values at half height of the second steps are approximately the same before and after the cutting process. This leads to believing that this step thus arises from adsorption on the same sites in both cases, namely the external convex surface of bundles. For each gas, the height of the second step is smaller on the cut SWNTs (Fig.4a); the height ratio before and after cutting is the same whatever the gas: $H_1/H_2 = 0.7 \pm 0.1$. This can be assigned to loss of external surface area of tubes resulting from introducing impurities upon cutting the tubes. On a weight basis, $30 \pm 5\%$ impurities were introduced by this opening treatment.

By normalizing the isotherms to the weight of tubes contained in the sample taking into account the percentage of impurities, we can compare quantitatively the results before and after the cutting process. Figure 4b displays isotherms normalized to the weight of nanotubes in the sample. The adsorbed amount increases significantly after the cutting process. Evidence is thus given of the accessibility of the insides of tubes to Kr, Xe and CCl_4 . The adsorbed amount inside the tubes can then be estimated from the isotherms (see table I).

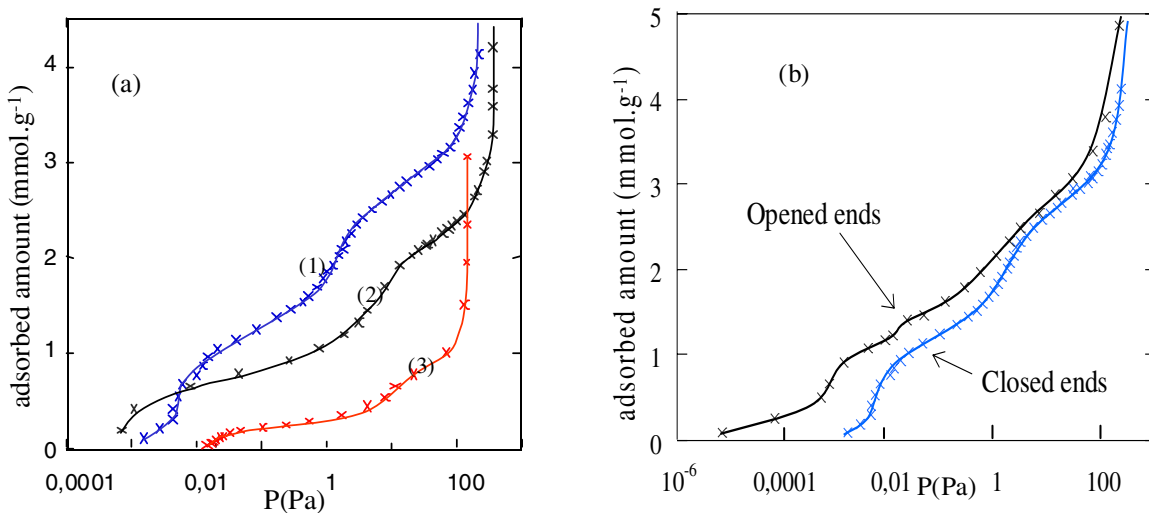


Figure 3: (a) Adsorption isotherms of (1) Kr at 77 K, (2) Xe at 110 K and (3) CCl_4 at 224 K, (b) Adsorption isotherms of Kr at 77 K on closed and opened SWNTs.

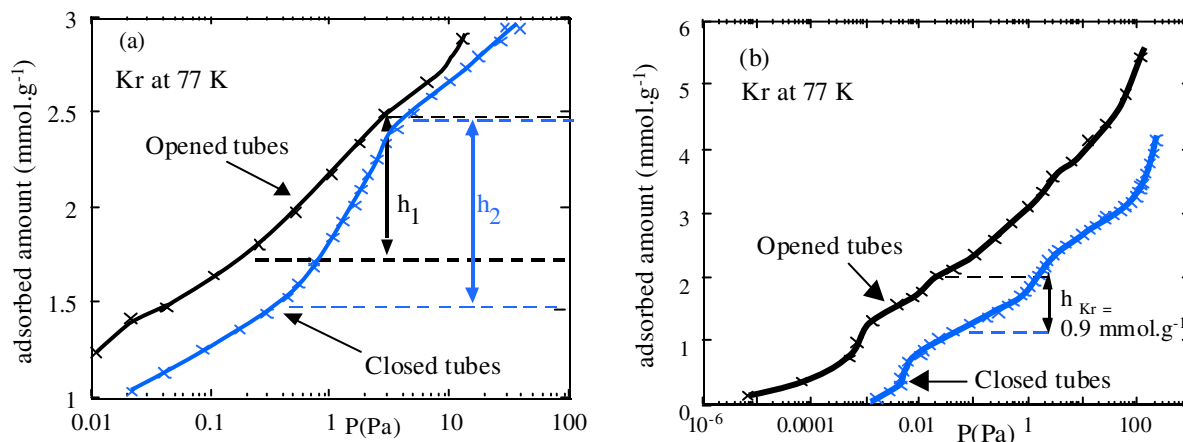


Figure 4: (a) Second step of Kr adsorption on closed and opened SWNTs, (b) Kr adsorption per nanotube weight in the sample before and after tube opening.

If we suppose that the gas molecules form 1D chains inside the tubes, the ratio of molecular diameters is not equal to the inverse of the corresponding ratios of adsorbed amounts inside the tubes, thus suggesting that the molecular arrangements are not the same for the three gases.

Table I. Adsorbate molecular diameter (D) and amount adsorbed inside the tubes after opening.

Gas	Kr	Xe	CCl ₄
D(nm)	0.406	0.448	0.598
V(mmol/g)	0.9 ± 0.1	0.6 ± 0.1	0.25 ± 0.1

Krypton adsorption on pristine MWNTs and on opened MWNTs:

Figure 5a (lower curve) displays the adsorption isotherm of Kr at 77.3 K on pristine MWNTs. The isotherm exhibits two steps of approximately the same height, both corresponding, as mentioned above, to adsorption on the uniform or quasi-uniform patches of the surface [7,8] namely the external walls of the nanotubes. These steps are not vertical nor is the plateau between the two steps completely horizontal. No hysteresis is observed between adsorption and desorption, which is consistent with TEM observation which show that the tubes in a pristine sample are closed. This implies that no capillary condensation takes place in the cavities formed by the isolated MWNTs.

In the case of oxidized MWNTs, the step becomes significantly wider (figure 5a, upper curve). Compared with the pristine MWNTs, the step height which is proportional to the uniform patches of the surface (when amorphous carbon does not contribute to the step-like adsorption), decreases after oxidation. However, a second step cannot be distinguished. Such a second step is thought to be more sensitive to surface crystallinity due to the low adsorbent-adsorbate interactions. This demonstrates that the oxidation generates a number of defects on the surface and thus an increase in superficial heterogeneity. In fact, the increase of Kr adsorption at very low pressures might be assigned to the creation of microporosity and other attractive sites. The plateau between the two steps became inclined, and a small hysteresis is observed. This reveals the opening of a number of tubes as observed by TEM. The hysteresis is small and thus cannot be taken as confirmation that the totality of the inner surface is accessible to Kr molecules. The BET specific surface area has increased after the oxidative treatment. By taking 15.7 Å² as the

molecular cross-section of Kr, we obtain $S_1 = 172 \text{ m}^2/\text{g}$ for the pristine sample, and $S_2 = 316 \text{ m}^2/\text{g}$ after oxidation.

Figure 5b shows the adsorption isotherms of Kr at 77.3 K on oxidized MWNTs after 40% and 60% burn-off. The isotherm shape does not vary with the percent of burn off. This observation allows proposing that the CO_2 attack proceeds by consumption of the tubes following their axes. After opening the tubes, the extremities became more reactive than the external walls.

What is the influence of curvature on the adsorption properties?

When we compare the adsorption isotherms of Kr on CNTs and on graphite under the same conditions, many differences are observed. First, the condensation pressure on nanotubes is higher than on graphite. As the second step on SWNTs is thought to represent adsorption on the convex surfaces of bundles and by taking into account the average CNT diameters in both SWNTs and MWNTs, we find that the narrower the diameter, the higher the condensation pressure (Table II). This is probably related mainly to the curvature of the graphene sheets. Furthermore, only two steps can be distinguished on the adsorption isotherm on CNTs instead of five on graphite. This may be a consequence of either (a) a displacement of condensation transitions toward higher pressures, or (b) the formation of more than two monolayers for MWNTs and more than one monolayer for SWNTs, but occurring at pressures near the Kr saturated vapor pressure and thus not visible on the isotherm.

Another difference concerns the slopes of the steps which are vertical with graphite but not with CNTs. Masenelli-Varlot *et al.* [7], suggested that this may be a consequence of the large dispersion in diameters; however, such is not the case for SWNTs for which the diameter dispersion is very narrow. Impurities and surface defects may also lead to step inclination. Clarification of these phenomena requires high purity CNT samples.

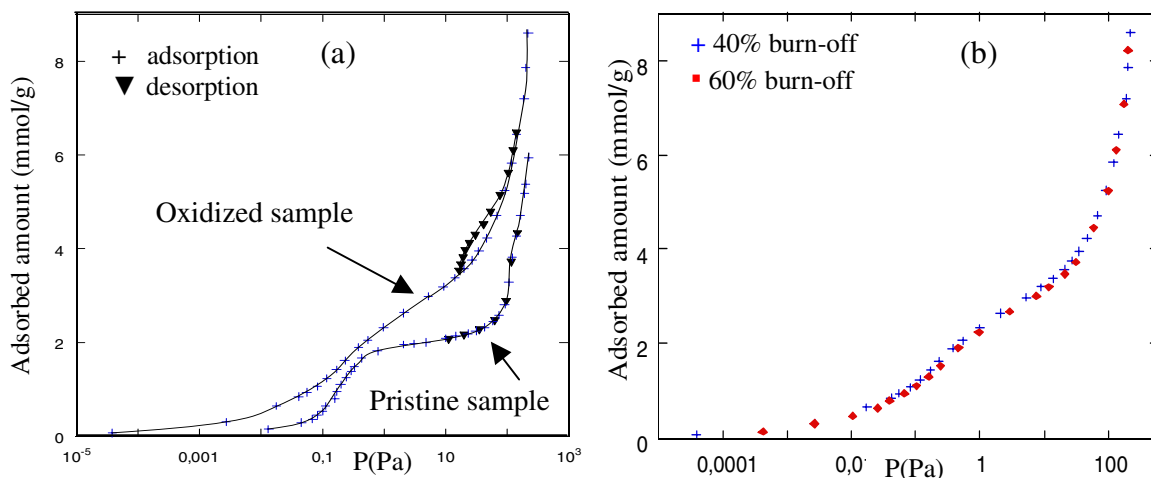


Figure 5. (a) Adsorption isotherm of Kr at 77.3 K on pristine MWNTs and on oxidized MWNTs after 40% burn-off.
 (b) Adsorption isotherms on oxidized MWNTs for 40% and 60% burn-off.

Table II. Half height step pressures of Kr adsorption isotherm at 77 K on external walls of MWNTs (10-45 nm), SWNTs (around 1.3 nm) and first step pressure on graphite.

Adsorbent	Graphite	MWNTs	SWNTs
P (Pa)	0.066	0.172	1.26
Ref.	[7]	This work	This work

CONCLUSIONS

Through the combined use of transmission electron microscopy and volumetric adsorption, this work has clearly shown that different processes can be used for efficient tube opening.

ACKNOWLEDGMENTS

The authors gratefully acknowledge financial support from the French ADEME (convention ADEME 01 74 042).

REFERENCES

1. P.M. Ajayan and S. Iijima, *Nature* **361**, 333-334 (1993).
2. M. Terrones, N. Grobert, W.K. Hsu, Y.Q. Zhu, W.B. Hu, H. Terrones, J.P. Hare, H.W. Kroto and D.R.M. Walton, *Bull. MRS.* **24**, 43-49 (1999).
3. J. Hu, T.W. Odom and C.M. Lieber, *Acc. Chem. Res.* **32**, 435-445 (1999).
4. M. Muris, M. Bienfait, P. Zeppenfeld, N. Dupont-Pavlovsky, M. Johnson, O.E. Vilches, T. Wilson, *Appl. Phys. A* **74**, S1293-S1295 (2002).
5. M. Muris, N. Dupont-Pavlovsky, M. Bienfait and P. Zeppenfeld. *Surf. Sci.* **492**, 67-74 (2001).
6. M.R. Babaa, I. Stepanek, K. Masenelli-Varlot, N. Dupont-Pavlovsky, E. McRae, and P. Bernier. *Surf. Sci.* **531**, 86-92 (2003).
7. K. Masenelli-Varlot, E. McRae and N. Dupont-Pavlovsky. *Appl. Surf. Sci.* **196**, 209-215 (2002).
8. A. Bougrine, N. Dupont-Pavlovsky, J. Ghanbaja, D. Billaud, and F. Beguin, *Surf. Sci.* **506**, 137-144 (2002).
9. A. Thomy, X. Duval and J. Regnier, *Surf. Sci. Rep.* **1**, 1-38 (1981).
10. T. Takaishi and S. Sensui. *Trans. Faraday. Soc.* **59**, 2503-14 (1963).
11. C. Journet, W.K. Maser, P. Bernier, A. Loiseau, M. Iamy de la Chapelle, S. Lefrant, P. Deniard, R. Lee and J.F. Fischer, *Nature.* **388**, 756-758 (1997).
12. I. Stepanek, G. Maurin, P. Bernier, J. Gavillet, A. Loiseau, R. Edwards and O. Jaschinski. *Chem. Phys. Lett.* **331**, 125-131 (2000).
13. S. Delpeux, K. Szostak, E. Frackowiak, S. Bonnamy; F. Beguin, *J. Nanosci. Nanotechnol.* **2**, 481-484 (2002).
14. F. Béguin, S. Delpeux-Ouldriane, K. Szostak, French Patent fr 0210115 (8 August 2002).